Table VII. Barriers to Internal Rotation in Phosphines and Phosphine-Borane Adducts

Compd	Barrier/(cal/mol)		Ref
	CH_3	BH_3	
CH_3PH_2	1960		20
$CH_3PH_2 \cdot BH_3$	2490	1570	29
$PH_3 \cdot BH_3$		2470	6
$PF_3 \cdot BH_3$		3240	3
CH_3PF_2	2300		11
$CH_3PF_2 \cdot BH_3$	>2000	>2000	This work
$HPF_2 \cdot BH_3$		3600–4500	4

shortening of the bond lengths between the phosphorus atom and its attached atoms and also by a flattening of the pyramid of which the phosphorus atom is the apex. The limited structural data on $CH_3PF_2 \cdot BH_3$ are consistent with these two general observations. The P–B bond lengths seem to fall into two groups, greater than 1.90 Å when hydrogen atoms or methyl groups are bonded to the phosphorus and about 1.84 Å when fluorine atoms are attached to the phosphorus. The data on $CH_3PF_2 \cdot BH_3$ also exhibit this effect. These observations about the structures of phosphine–borane adducts have been made before.[5] They are repeated here to show that the data for $CH_3PF_2 \cdot BH_3$ are consistent with the data for other members of this class of compounds. The structure changes which occur in the phosphine upon adduct formation are consistent with the predictions of elementary bonding models, whereas there seems to be no uniquely compelling explanation for the variation of the observed P–B bond lengths and stabilities of the adducts.[5] While this study of the structure of $CH_3PF_2 \cdot BH_3$ is by no means complete, the results do not appear to support the speculation of Foester and Cohn[10] concerning an unusual structural deformation in CH_3PF_2 upon adduct formation.

Table VII summarizes barriers to internal rotation in related compounds. The absence of resolvable splittings in the ground vibrational state of $CH_3PF_2 \cdot BH_3$ places lower limits of about 2000 cal/mol on both the CH_3 and BH_3 barriers to internal rotation. In CH_3PH_2 formation of the BH_3 adduct has increased the barrier to CH_3 internal rotation by 530 cal/mol, and in $PH_3 \cdot BH_3$ the substitution of a methyl group on the phosphorus has lowered the barrier to BH_3 group internal rotation by 900 cal/mol. Similar changes applied to the data on CH_3PF_2 and PF_2BH_3 predict values of 2830 and 2340 cal/mol, respectively, for CH_3 and BH_3 group internal rotation barriers in the present compound. These predictions are quite crude, but they do serve to show that the experimental observation that both barriers in the present compound are greater than 2000 cal/mol is consistent with the data on related compounds.

Registry No. $CH_3PF_2 \cdot {}^{11}BH_3$, 55606-68-3; $CH_3PF_2 \cdot {}^{11}BD_3$, 55606-69-4; $CH_3PF_2 \cdot {}^{10}BH_3$, 55606-70-7; $CH_3PF_2 \cdot {}^{10}BD_3$, 55606-69-4.

References and Notes

(1) This work was supported in part by grants from the National Science Foundation.
(2) A preliminary account of this work was presented at the Symposium on Molecular Structure and Spectroscopy, Columbus, Ohio, June 1974.
(3) R. L. Kuczkowski and D. R. Lide, Jr., *J. Chem. Phys.*, **46**, 357 (1967).
(4) J. P. Pasinski and R. L. Kuczkowski, *J. Chem. Phys.*, **54**, 1903 (1971).
(5) P. S. Bryan and R. L. Kuczkowski, *Inorg. Chem.*, **11**, 553 (1972).
(6) J. R. Durig, Y. S. Li, L. A. Carriera, and J. D. Odom, *J. Am. Chem. Soc.*, **95**, 2491 (1973).
(7) J. D. Odom, B. A. Hudgens, and J. R. Durig, *J. Phys. Chem.*, **77**, 1972 (1973).
(8) J. D. Odom, S. Riethmiller, S. J. Meischen, and J. R. Durig, *J. Mol. Struct.*, **20**, 471 (1974).
(9) J. R. Durig, B. A. Hudgens, Y. S. Li, and J. D. Odom, *J. Chem. Phys.*, **61**, 4890 (1974).
(10) R. Foester and K. Cohn, *Inorg. Chem.*, **11**, 2590 (1972).
(11) E. G. Codding, R. A. Creswell, and R. H. Schwendeman, *Inorg. Chem.*, **13**, 856 (1974).
(12) A. H. Brittain, J. E. Smith, P. L. Lee, K. Cohn, and R. H. Schwendeman, *J. Am. Chem. Soc.*, **93**, 6772 (1971).
(13) A. H. Brittain, J. E. Smith, and R. H. Schwendeman, *Inorg. Chem.*, **11**, 39 (1972).
(14) P. L. Lee, K. Cohn, and R. H. Schwendeman, *Inorg. Chem.*, **11**, 1917 (1972).
(15) E. G. Codding, C. E. Jones, and R. H. Schwendeman, *Inorg. Chem.*, **13**, 178 (1974).
(16) F. J. Wodarczyk and E. B. Wilson, *J. Mol. Spectrosc.*, **37**, 445 (1971).
(17) J. S. Muenter, *J. Chem. Phys.*, **48**, 4544 (1968).
(18) R. H. Schwendeman, in "Critical Evaluation of Chemical and Physical Structural Information", D. R. Lide, Jr., and M. A. Paul, Ed., National Academy of Sciences, Washington, D.C., 1974, Chapter III.3.
(19) L. S. Bartell, *J. Chem. Phys.*, **32**, 832 (1960).
(20) T. Kojima, E. L. Breig, and C. C. Lin, *J. Chem. Phys.*, **35**, 2139 (1961).
(21) C. A. Burrus, *J. Chem. Phys.*, **28**, 427 (1958).
(22) R. Nelson, *J. Chem. Phys.*, **39**, 2382 (1963).
(23) D. R. Lide and D. E. Mann, *J. Chem. Phys.*, **29**, 914 (1958).
(24) R. L. Kuczkowski, *J. Am. Chem. Soc.*, **90**, 1705 (1968).
(25) S. N. Ghosh, R. Trambarulo, and W. Gordy, *J. Chem. Phys.*, **21**, 308 (1953).
(26) P. S. Bryan and R. L. Kuczkowski, *J. Chem. Phys.*, **55**, 3049 (1971).
(27) Y. Morino, K. Kuchitsu, and T. Moritani, *Inorg. Chem.*, **8**, 867 (1969).
(28) C. A. Burrus, A. Jache, and W. Gordy, *Phys. Rev.*, **95**, 706 (1954).
(29) J. R. Durig, V. F. Kalasinsky, Y. S. Li, and J. D. Odom, *J. Phys. Chem.*, **79**, 468 (1975).

Contribution from the Technical University of Denmark,
Chemistry Department A, DK-2800 Lyngby, Denmark

Lower Oxidation States of Selenium. I. Spectrophotometric Study of the Selenium–Selenium Tetrachloride System in a Molten NaCl–$AlCl_3$ Eutectic Mixture at 150°

R. FEHRMANN, N. J. BJERRUM,* and H. A. ANDREASEN

Received February 4, 1975

AIC500756

Four different solvated selenium species with low positive oxidation states were prepared by reduction of dilute solutions of $SeCl_4$ in a NaCl–$AlCl_3$ (37:63 mol %) melt at 150° with elementary selenium. A statistical analysis of the spectrophotometric measurements of the resulting melts showed that the two higher oxidation states of these species were $+^1/_2$ and $+^1/_4$ (or $+^4/_{17}$) whereas no accurate value could be calculated for the two lower oxidation states. The most likely values, however, of these lower oxidation states were found to be $+^1/_6$ and $+^1/_8$. Spectra for the possible species $Se_4{}^{2+}$, $Se_8{}^{2+}$, $Se_{12}{}^{2+}$, and $Se_{16}{}^{2+}$ were also calculated.

Introduction

It has been known for a long time that selenium in analogy with tellurium forms colored solutions in sulfuric acid.[1] A fairly recent investigation by Gillespie and coworkers has revealed that these colored solutions contain the $Se_4{}^{2+}$ and $Se_8{}^{2+}$ ions.[2] The results obtained by Corbett and coworkers[3] seem to indicate that the same two ions are formed in chloroaluminate melts. The structure of $Se_4{}^{2+}$ in $Se_4(HS_2O_7)_2$ is square planar[4] and the structure of $Se_8{}^{2+}$ in $Se_8(AlCl_4)_2$ is bicyclic.[5] In the present work the solute selenium species in a NaCl–$AlCl_3$

(37:63 mol %) melt are examined spectrophotometrically and an attempt is made to determine the oxidation states of the four species formed.

Experimental Section

Materials. $AlCl_3$ was made from the pure metal (99.999%) and HCl gas (made by reaction between concentrated hydrochloric acid and concentrated sulfuric acid) and further purified by sublimation. NaCl (analytical reagent from Riedel-de Haën) was purified by first passing HCl gas (electronic grade from Matheson) over the solid and then through the melt, flushing with pure N_2, and finally filtering the melt. The $SeCl_4$ was made by reaction between selenium (99.999%) and chlorine (Fluka >99.9%) and further purified by sublimation in chlorine gas. An analysis of the final product gave as an average of five measurements a chlorine content of 64.44 ± 0.25%. The theoretical value for $SeCl_4$ is 64.23%.

The materials that made up a melt were weighed in a nitrogen-filled glove box, where the water content was ca. 5 ppm. To avoid decomposition of the used $SeCl_4$ (to Se_2Cl_2 and Cl_2) the crystalline $SeCl_4$ was kept in small sealed glass tubes until used. Furthermore after the cell was sealed under $^1/_3$ atm nitrogen, no further addition was made to the melt.

Measurements. The optical cells were of fused quartz (Ultrasil from Helma) and had known path lengths of either ca. 0.5 mm or ca. 0.1 mm. The path lengths of about 0.1 mm were obtained by placing precision-ground fused-silica inserts into 5-mm cells. The spectra were measured with a Cary 14R spectrophotometer equipped with a furnace similar in shape to the furnace described previously[6] but with an independent temperature regulation of the horizontal tube. This furnace was regulated to within ±0.1° at 150° by a Eurotherm regulator, Type LP96/DHS/PID/P. The temperature of the furnace was measured by a calibrated chromel–alumel thermocouple connected to a type DM 2022S digital voltmeter from Digital Measurements Ltd. with a built-in standard cell. The spectrophotometer was equipped with a Datex digital system for punching out spectral data on paper tape.

In order to get reproducible results the charged cell was placed in a Kanthal wire wound quartz tube furnace (surrounded by a water-cooled glass jacket) and was gently rocked over an extended period of time (16–72 hr). After this treatment the optical cell was placed in the spectrophotometric furnace, where it was kept from 2 to 24 hr before the spectra were recorded.

Results and Discussion

General Considerations. The initial molar amount of one of the added substances (in the present work NaCl, $AlCl_3$, Se, and $SeCl_4$) dissolved in 1 l. of the melt is defined as its formality. The formal absorptivity is defined by $A(lc')^{-1}$, where A is the absorbance corrected for the absorbance of cell and solvent, l is the path length, and c' is the formality. The densities of the solutions were calculated assuming ideal mixtures of Se, $SeCl_4$, and NaCl–$AlCl_3$. This assumption will only give rise to a small error, as the amounts of Se and $SeCl_4$ added were small compared to the amounts of NaCl–$AlCl_3$. The densities of Se and NaCl–$AlCl_3$ were obtained from the work of Dobinski and Wesolowski[7] and Boston,[8] respectively. No value was found in the literature for the density of molten $SeCl_4$; instead it was assumed that the relative expansion in going from the solid at room temperature to the molten state at 150° was the same for both $SeCl_4$ and $TeCl_4$. The density of molten $TeCl_4$ at 150° was found by extrapolation of the density data given by Simons.[9] The densities of solid $TeCl_4$ and solid $SeCl_4$ were taken from the work by Hönigschmid and Baudrexler[10] and Shoemaker and Abrahams,[11] respectively.

The Bourguer–Beer law as well as the law of additive absorbance was assumed to be valid. It was also assumed that the activity coefficients did not vary. This can be justified by the fact that the ionic strength of the solvent was high and not expected to change much by addition of small amounts of solute ions. Due to the reaction $Al_2Cl_7^- + Cl^- \rightleftharpoons 2AlCl_4^-$ [12–15] the melt was well buffered with respect to the chloride activity.

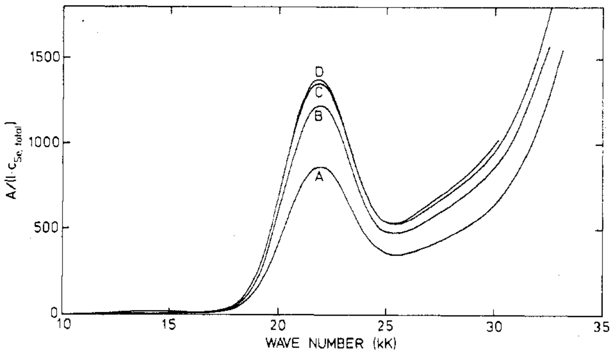

Figure 1. Series of spectra of solutions of $SeCl_4$ reduced with selenium. Se:$SeCl_4$ formality ratio and formality of $SeCl_4$, respectively: A, 1.30, 0.02421; B, 3.85, 0.01757; C, 5.69, 0.01127; D, 7.04, 0.02027. Solvent is NaCl-$AlCl_3$ (37:63 mol %) at 150°.

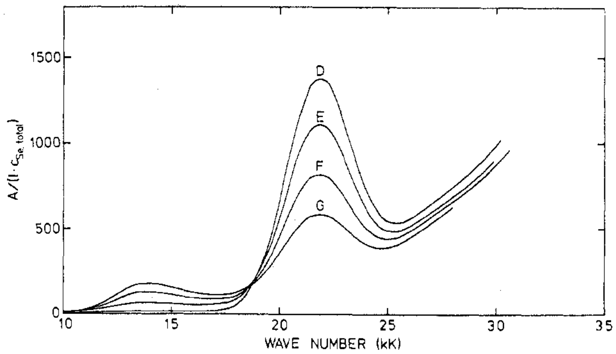

Figure 2. Series of spectra of solutions of $SeCl_4$ reduced with selenium. Se:$SeCl_4$ formality ratio and formality of $SeCl_4$, respectively: D, 7.04, 0.02027; E, 7.92, 0.01926; F, 9.56, 0.01366; G, 10.98, 0.02199. Solvent is NaCl-$AlCl_3$ (37:63 mol %) at 150°.

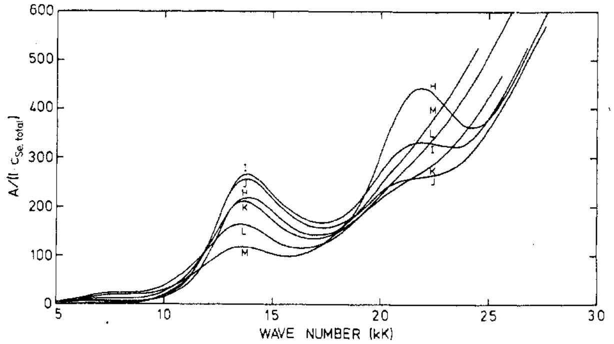

Figure 3. Series of spectra of solutions of $SeCl_4$ reduced with selenium. Se:$SeCl_4$ formality ratio and formality of $SeCl_4$, respectively: H, 12.48, 0.01545; I, 14.07, 0.03372; J, 15.00, 0.01784; K, 17.35, 0.03123; L, 19.23, 0.01338; M, 21.29, 0.02301. Solvent is NaCl-$AlCl_3$ (37:63 mol %) at 150°.

Species Formed in the NaCl–$AlCl_3$ Eutectic. If small amounts of selenium are added to a dilute solution of $SeCl_4$ in NaCl–$AlCl_3$ (37:63 mol %) at 150°, colored solutions are obtained. A survey of the spectra of these solutions is shown in Figures 1–4. In order to compare the spectra measured at different formal concentrations of $SeCl_4$ and selenium, the absorptivities have all been divided by the total concentration of selenium (i.e., the formal concentration of $SeCl_4$ plus the formal concentration of selenium). This is expressed in the formulation $A/lc_{Se,total}$, where A and l have the meanings given above and $c_{Se,total}$ is the total concentration of selenium. The spectra are conveniently divided into four ranges determined by the formality ratio of Se:$SeCl_4$ (i.e., the formal concentration of selenium divided by the formal concentration of $SeCl_4$). In the formality ratio range 0–7 shown in Figure 1 only one

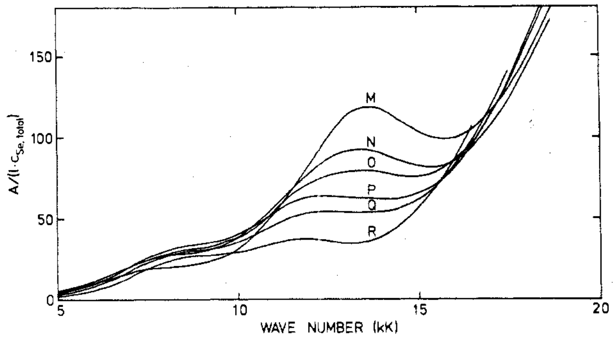

Figure 4. Series of spectra of solutions of $SeCl_4$ reduced with selenium. Se:$SeCl_4$ formality ratio and formality of $SeCl_4$, respectively: M, 21.29, 0.02301; N, 23.03, 0.01347; O, 24.14, 0.01328; P, 25.89, 0.01057; Q, 27.14, 0.01435; R, 31.05, 0.01601. Solvent is NaCl-$AlCl_3$ (37:63 mol %) at 150°.

species is formed by the reduction of $SeCl_4$ by selenium. This can be verified by the observation that the Bourguer–Beer law with respect to the formality of selenium was followed at all the measured wavelengths (Se(IV) absorbs only in the ultraviolet part of the spectrum) and that changes in the temperature over the range 150–200° produced only minor changes in the spectrum characterized by a peak at 21.9 kK. For convenience this reaction product will be labeled I. The formation of only one reaction product is in agreement with the change in the spectra shown in Figure 1. As more and more of the Se(IV) is reduced forming I, $A/lc_{\text{Se,total}}$ approaches the spectrum of I in terms of formal absorptivity vs. wave number.

If the formality ratio Se:$SeCl_4$ is increased to values higher than 7, the peak at 21.9 kK begins to decrease. This is shown in Figure 2 for the range 7–11. As seen from this figure, the curves D–G form an isosbestic point located at 18.8 kK. A closer analysis of the spectra shows that these are internally linearly dependent.[16] This suggests that two reaction products are present and for convenience the additional species with a peak at 13.8 kK will be labeled II.

For formality ratios from 11 to 31 it is not possible to obtain a two-species equilibrium. It is convenient, however, to divide this range into two new ranges. Figure 3 shows the spectra in the range 12–20. What can be observed here is a decrease of the peak at 21.9 kK (due to I) and an increase and then a decrease of the peak at 13.8 kK (due to II) followed by an apparent shift to a band at 13.3 kK. This shift is accompanied by an increase in $A/lc_{\text{Se,total}}$ at 8.4 kK and at wave numbers higher than ca. 17 kK. Since the increase at 8.4 kK and at wave numbers higher than ca. 17 kK seems to follow the shift to 13.3 kK, it is reasonable to expect that only one additional species is present. This species will be labeled III. Figure 4 shows the spectra for the Se:$SeCl_4$ formality range 21–31. What can be observed here is a decrease of the band at 13.3 kK (due to III) and an apparent shift to a band located at 11.8 kK and at the same formality ratios first an increase and then a decrease in $A/lc_{\text{Se,total}}$ at 8.4 kK followed by an apparent shift to a band at 8.8 kK. The entity with bands at 11.8 and 8.8 kK will be labeled IV.

Another way of viewing the obtained results is shown in Figure 5. Here the formal absorptivities of $SeCl_4$ measured at two wave numbers 21.9 and 13.9 kK are plotted vs. the Se:$SeCl_4$ formality ratio. It can be shown from the Bouguer–Beer law, the law of additive absorbances, and the mass action relation that straight lines on such a plot—straight lines which furthermore are independent of the total concentration—can only be obtained if two species are present. Based on this information it is possible to say that in the formality ratio range 0–7 only two species are present (Se(IV) and I) since the formal concentration of selenium is varied 2.1 times without any significant variation from the straight line. Correspondingly only two species (I and II) are present in the range 7–11.5. The formal concentration of $SeCl_4$ is here varied 1.7 times, and finally only two species (II and III) are present in the formality ratio range 19.5–22. The formal concentration in the last range is varied 1.7 times.

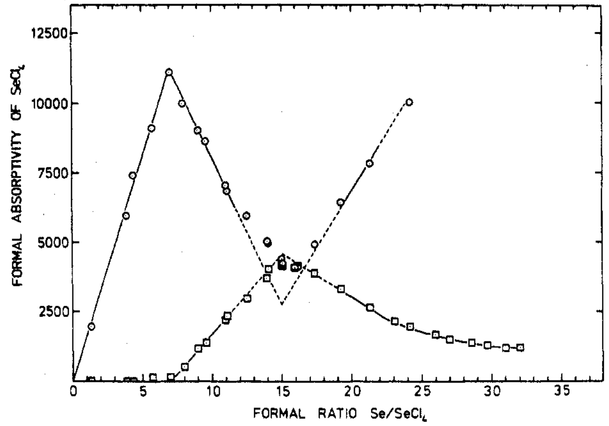

Figure 5. Relation between the formal absorptivity of $SeCl_4$ and the Se:$SeCl_4$ formality ratio measured at two different wave numbers: circles, at 21.9 kK; squares, at 13.9 kK.

In the range very close to 7, in the range 11–19.5, and in the range 22–31 three species equilibria must be present. After the formality ratio 31 is reached the spectra do not change. This must mean that the solution is now saturated with selenium. The solubility of selenium in pure NaCl–$AlCl_3$ eutectic was found to be very low. Equilibration of a small piece of selenium (ca. 3 mg) with about 7 ml of melt at 150° for 2–4 days gave a weight loss of ca. 1 mg. The solubility was in this way determined in two experiments to be 0.0015 and 0.0022 mol/l.

Determination of Oxidation States in NaCl–$AlCl_3$ Eutectic. From the above discussion it is clear that only two species, Se(IV) and I, are present, as long as the Se:$SeCl_4$ formality ratio is less than about 7. As the formality Se:$SeCl_4$ ratio is increased toward 7, the concentration ratio Se(IV):I must decrease until Se(IV) disappears at a Se:$SeCl_4$ formality ratio of about 7. If the correct value is 7, then the reaction

$$7\text{Se} + \text{Se}^{4+} \rightarrow (4/n)\text{Se}_{2n}{}^{n+} \qquad (n = 1, 2, 3, \ldots) \tag{1}$$

continues until all Se(IV) is consumed and the added selenium starts to reduce $Se_{2n}{}^{n+}$ forming II. The oxidation state of I must then be $+{}^1/_2$. Based on Figure 5 there seems to be no doubt that the correct value for the first break is 7. Since the formality ratios for the other breaks in Figure 5 are not as well defined, we decided to treat the data in all the formality ranges with model reactions of the form

$$h\text{Se}_q{}^{r+} + j\text{Se}_v{}^{x+} \rightleftarrows k\text{Se}_y{}^{z+} \tag{2}$$

where h, j, k, q, r, v, x, y, and z are integers. The limitation for the models was that charges higher than 4+ were not used. A survey of the chemical literature shows that few compounds have a positive charge higher than 4+. More common seem to be anions with negative charges smaller than 4− (i.e., numerical values higher than 4) found in polymolybdates and polytungstates. In the formality range 0–11.5 $Se_q{}^{r+}$ will then have to represent Se^{4+} and $Se_y{}^{z+}$ and $Se_v{}^{x+}$ will have to represent I and II, respectively. The second break on the curves in Figure 5 is close to the formality ratio 15, corresponding to the formation of a species with oxidation state $+{}^1/_4$, and since Corbett and coworkers[5] have proved the existence of $Se_8{}^{2+}$ in solid $Se_8(AlCl_4)_2$, $Se_8{}^{2+}$ was selected to represent II in the calculation regarding I. Other formulas for II, with oxidation state close to $+{}^1/_4$, gave results not far from the results obtained for $Se_8{}^{2+}$. On the basis of the Bouguer–Beer

Table I. Variances Obtained for Models[a] with Oxidation States Close to $+{}^{1}/_{2}$[b]

	Formal charge			
Oxidn state	1+	2+	3+	4+
$+{}^{2}/_{3}$		1.15×10^{-2}		1.14×10^{-2}
$+{}^{3}/_{5}$			2.21×10^{-3}	
$+{}^{4}/_{7}$				1.65×10^{-3}
$+{}^{1}/_{2}$	5.01×10^{-4}*	5.01×10^{-4}*	5.01×10^{-4}*	5.01×10^{-4}*
$+{}^{4}/_{9}$				5.41×10^{-3}
$+{}^{3}/_{7}$			7.22×10^{-3}	
$+{}^{2}/_{5}$		1.49×10^{-2}		1.54×10^{-2}

[a] Other species in the equilibria assumed to be Se^{4+} and $Se_8{}^{2+}$. [b] Number of spectra 10; number of different wave numbers 391; formality ratio range 1.30–11.11.

Table II. Variances Obtained for Models[a] with Oxidation States Close to $+{}^{1}/_{4}$[b]

	Formal charge			
Oxidn states	1+	2+	3+	4+
$+{}^{2}/_{7}$		7.31×10^{-3}		7.30×10^{-3}
$+{}^{3}/_{11}$			4.57×10^{-3}	
$+{}^{4}/_{15}$				3.53×10^{-3}
$+{}^{1}/_{4}$	1.25×10^{-3}*	1.29×10^{-3}*	1.43×10^{-3}*	1.51×10^{-3}*
$+{}^{4}/_{17}$				1.45×10^{-3}*
$+{}^{3}/_{13}$			2.33×10^{-3}*	
$+{}^{2}/_{9}$		3.23×10^{-3}		4.76×10^{-3}
$+{}^{3}/_{14}$			5.52×10^{-3}	

[a] Other species in the equilibria assumed to be $Se_4{}^{2+}$ and $Se_{12}{}^{2+}$. [b] Number of spectra 14; number of different wave numbers 391; formality ratio range 9.02–21.29.

Table III. Variances Obtained for Models[a] with Oxidation States in the Range $+{}^{1}/_{4}$–$+{}^{1}/_{8}$[b]

	Formal charge			
Oxidn states	1+	2+	3+	4+
$+{}^{1}/_{4}$[c]				
$+{}^{4}/_{17}$				5.38×10^{-4}*
$+{}^{3}/_{13}$			6.62×10^{-4}*	
$+{}^{2}/_{9}$		8.08×10^{-4}*		8.74×10^{-4}*
$+{}^{3}/_{14}$			1.63×10^{-3}	
$+{}^{4}/_{19}$				7.85×10^{-4}*
$+{}^{1}/_{5}$	6.22×10^{-4}*	1.61×10^{-3}	1.04×10^{-3}*	1.60×10^{-3}
$+{}^{4}/_{21}$				9.95×10^{-4}*
$+{}^{3}/_{16}$			1.64×10^{-3}	
$+{}^{2}/_{11}$		6.54×10^{-4}*		1.50×10^{-3}*
$+{}^{3}/_{17}$			1.29×10^{-3}*	
$+{}^{4}/_{23}$				1.21×10^{-3}*
$+{}^{1}/_{6}$	5.15×10^{-4}*	6.44×10^{-4}*	7.85×10^{-4}*	8.49×10^{-4}*
$+{}^{4}/_{25}$				5.58×10^{-4}*
$+{}^{3}/_{19}$			5.19×10^{-4}*	
$+{}^{2}/_{13}$		5.07×10^{-4}*		5.07×10^{-4}*
$+{}^{3}/_{20}$			5.49×10^{-4}*	
$+{}^{4}/_{27}$				5.72×10^{-4}*
$+{}^{1}/_{7}$	6.94×10^{-4}*	7.25×10^{-4}*	7.32×10^{-4}*	7.32×10^{-4}*
$+{}^{4}/_{29}$				8.07×10^{-4}*
$+{}^{3}/_{22}$			8.68×10^{-4}*	
$+{}^{2}/_{15}$		1.00×10^{-3}*		1.00×10^{-3}*
$+{}^{3}/_{23}$			1.22×10^{-3}*	
$+{}^{4}/_{31}$				1.25×10^{-3}*
$+{}^{1}/_{8}$[c]				

[a] Other species in the equilibria assumed to be $Se_8{}^{2+}$ and $Se_{16}{}^{2+}$. [b] Number of spectra 9; number of different wave numbers 233; formality ratio range 21.29–31.05. [c] Variance cannot be calculated.

law it can be shown that if we deal with m different spectra obtained at different compositions, a general equation involving three matrices can be put forward, i.e.

$$[l_m c_{mi}][\epsilon_i(\nu_n')] = [A_m(\nu_n')] \qquad (3)$$

where l_m is the path length at the mth composition, c_{mi} is the concentration of the ith species for the mth composition, $\epsilon_i(\nu_n')$ is the molar absorptivity of the ith species at the wave number ν_n', and $A_m(\nu_n')$ is the total absorbance of the mth composition at the wave number ν_n'. This equation has recently been given in a slightly different form.[17] From the model put forward to explain the spectral changes of the melt and on the basis of an arbitrarily chosen equilibrium constant, the concentration of each species c_i is calculated. This (together with the measured absorbances at different wave numbers and different compositions) is now introduced in eq 3 and the "best" values of $\epsilon_i(\nu_n')$ (least squares) are calculated. By varying systematically the equilibrium constant the deviation (least squares) between the measured and calculated spectra is minimized. Calculations of this type have previously been performed by Lieto[18] and Conrow, Johnson, and Bowen.[19] The result of calculations for the formality ratio range 0–11.5 is shown in Table I. In order to save space only the variances have been given in this table. The 10 spectra were measured at 391 different wave numbers in the range 11.1–27.8 kK. To distinguish as well as possible between the different models

Table IV. Variances Obtained for Models[a] with Oxidation States in the Range $+^1/_7$–$^1/_{11}$[b]

	Formal charge			
Oxidn states	1+	2+	3+	4+
$+^1/_7$	4.41×10^{-3}	4.83×10^{-3}	6.33×10^{-3}	4.97×10^{-3}
$+^4/_{29}$				5.66×10^{-3}
$+^3/_{22}$			2.64×10^{-3}	
$+^2/_{15}$		2.65×10^{-3}		4.22×10^{-3}
$+^3/_{23}$			1.09×10^{-2}	
$+^4/_{31}$				6.14×10^{-3}
$+^1/_8$	3.41×10^{-4}*	3.41×10^{-4}*	5.37×10^{-4}*	3.41×10^{-4}*
$+^4/_{33}$				6.17×10^{-3}
$+^3/_{25}$			3.51×10^{-4}*	
$+^2/_{17}$		3.47×10^{-4}*		3.27×10^{-4}*
$+^3/_{26}$			3.48×10^{-4}*	
$+^4/_{35}$				7.72×10^{-3}
$+^1/_9$	6.02×10^{-4}*	3.57×10^{-4}*	3.77×10^{-4}*	2.60×10^{-4}*
$+^4/_{37}$				3.13×10^{-2}
$+^3/_{28}$			2.44×10^{-4}*	
$+^2/_{19}$		3.31×10^{-4}*		2.17×10^{-4}*
$+^3/_{29}$			4.59×10^{-4}*	
$+^4/_{39}$				3.13×10^{-2}
$+^1/_{10}$	7.84×10^{-4}	3.42×10^{-4}*	9.92×10^{-4}	6.00×10^{-4}*
$+^4/_{41}$				3.13×10^{-2}
$+^3/_{31}$			2.15×10^{-3}	
$+^2/_{21}$		4.50×10^{-3}		1.69×10^{-2}
$+^3/_{32}$			2.60×10^{-2}	
$+^4/_{43}$				3.13×10^{-2}
$+^1/_{11}$	4.52×10^{-3}	4.50×10^{-3}	4.48×10^{-3}	1.07×10^{-3}

[a] Other species in equilibria assumed to be Se_{12}^{2+} and Se_8^{2+}. [b] Number of spectra 9; number of different wave numbers 233; formality ratio range 24.14–32.04.

a smoothing out procedure has been applied to the spectra obtained in this range and in the other ranges. In this procedure the absorbance of the middle point of three successive points have been obtained by a linear least-squares interpolation.[20]

From the variance in Table I (calculated with respect to the deviation between the measured and calculated spectra at all wave numbers) it is clear that the oxidation states $+^1/_2$ (marked with asterisks) give better fits than any of the other oxidation states. In order to distinguish between the models we applied a so-called F test ($F = v_1/v_2$, where v is the variance)[21] to the results with the lowest obtained variance as the denominator and based the distinction on 10% probability points. Under these circumstances the oxidation state $+^1/_2$ was found to give a significantly better fit than any of the other oxidation states. It was here assumed that there were only as many degrees of freedom as there were different melt compositions minus 3. The reason for only looking at melt compositions and not at the total number of measured absorbances (as has been done in order to get the variances shown in Table I) was that these absorbances were not truly independent of each other, since they belonged in groups to particular formality ratios. The error in the formality ratios is mainly due to oxidizing or reducing impurities and not to weighing errors.

In Table II is shown the result of similar calculations for the formality ratio range 8–22. In these calculations the formulations Se_4^{2+} and Se_{12}^{2+} have been used for species I and III, respectively, but other formulations of these species, such as Se_2^+, Se_8^{4+}, Se_6^+, Se_{24}^{4+}, and Se_{26}^{4+}, will not change the general picture of the calculations shown in Table II as long as the oxidation states are kept close to $+^1/_2$ and $+^1/_6$. For the equilibria $2Se_2^+ + Se_{12}^{2+} \rightleftharpoons 2Se_8^{2+}$, $Se_8^{4+} + 2Se_{12}^{2+} \rightleftharpoons 4Se_8^{2+}$, $Se_4^{2+} + 2Se_6^+ \rightleftharpoons 2Se_8^{2+}$, $2Se_4^{2+} + Se_{24}^{4+} \rightleftharpoons 4Se_8^{2+}$, and $5Se_4^{2+} + 2Se_{26}^{4+} \rightleftharpoons 9Se_8^{2+}$, the variances 1.80×10^{-3}, 0.98×10^{-3}, 1.06×10^{-3}, 1.71×10^{-3}, and 1.79×10^{-3} were obtained, respectively. From the variances in Table II it is clear that the oxidation states $+^1/_4$ and $+^4/_{17}$ give better fits than any other oxidation states. If we apply an F test to results in the same way as done in the 0–11.5 formality ratio range, possible formulas for species II are Se_{4n}^{n+} (n = 1–4), Se_{13}^{3+}, and Se_{17}^{4+}. Each of these possibilities is marked with an asterisk in Table II.

In Table III is shown the result of a calculation for the formality ratio range 21–31. It has been assumed that the formula for II is Se_8^{2+} and that the formula for IV is Se_{16}^{2+}. Unfortunately as can be seen from this table the variances for all models in the oxidation state range from $+^1/_4$ to $+^1/_8$ are rather similar. An F test shows that few of the shown models can be excluded, but taken as a whole, the most likely value for the oxidation state of III seems to be $+^1/_6$. As before possible formulas for species III are marked with asterisks. The number of species considered in the analysis would be lessened if those with an odd number of electrons could be excluded. It is well-known that compounds with an odd number of electrons are not often found. However, the low oxidation states of sulfur (found in HSO_3F and oleum) in some cases give rise to ESR signals.[22] In view of this it is difficult to exclude completely selenium species with an odd number of electrons.

In Table IV is shown the result of a calculation for the formality ratio range 24–33. It has here been assumed that the formula for III is Se_{12}^{2+} and the formula for elementary selenium is Se_8. However, other formulas for the dissolved elementary selenium such as Se_2 or Se will not change the results significantly. For the equilibria $Se_{12}^{2+} + 2Se_2 \rightleftharpoons Se_{16}^{2+}$ and $Se_{12}^{2+} + 4Se \rightleftharpoons Se_{16}^{2+}$ the variances 3.40×10^{-4} and 3.28×10^{-4} were obtained, respectively. As shown in Table IV it is not possible to distinguish between many of the models on a basis of the given variances. The only thing that can be concluded is that the oxidation state of IV lies in the range $+^1/_8$–$+^1/_{10}$. Of all these values $+^1/_8$ is the most likely, not based on the present measurements but based on comparison with the work by Gillespie and coworkers[23] in which they isolated and characterized the sulfur compound $S_{16}(AsF_6)_2$ from anhydrous hydrogen fluoride. The problem is that the measured absorbances and especially the calculated formality ratios are not known accurately enough. Unfortunately we see at present no way of improving such data.

In the process of calculating the variance for the different

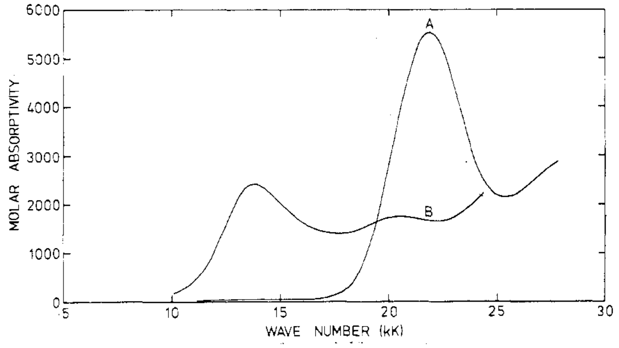

Figure 6. Calculated spectra of the models Se_4^{2+} (A) and Se_8^{2+} (B). Se_4^{2+} was calculated on basis of 10 measured spectra; Se_8^{2+} was calculated on basis of 14 measured spectra.

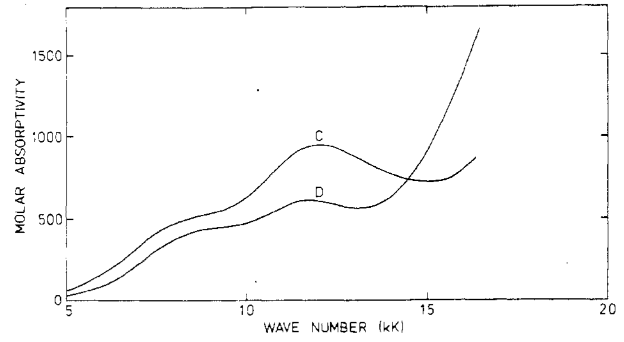

Figure 7. Calculated spectra of the models Se_{12}^{2+} (C) and Se_{16}^{2+} (D). Both Se_{12}^{2+} and Se_{16}^{2+} were calculated on basis of 9 measured spectra.

equilibria one obtains at the same time the spectra for all species in the equilibria. In Figures 6 and 7 are shown the calculated spectra of the models Se_4^{2+}, Se_8^{2+}, Se_{12}^{2+}, and Se_{16}^{2+}. The equilibrium constants for all of the model reactions described above are of course also calculated together with the variances, but since it is not possible to distinguish between many of the possible reactions, the equilibrium constants are not included in the present paper. However, by a newly developed potentiometric method[24] there seems to be hope to distinguish between different reactions. Under these circumstances it will be important to compare the equilibrium constants obtained by the spectrophotometric method with the constants obtained by the potentiometric method.

Acknowledgment. The authors wish to acknowledge the financial support of Statens teknisk-videnskabelige Forskningsrad. Further thanks are due to the Northern Europe University Computing Center (NEUCC) for computing time.

Registry No. Se, 7782-49-2; $SeCl_4$, 10026-03-6.

References and Notes

(1) G. Magnus, *Ann. Phys. (Leipzig)*, [2] **10**, 491 (1827).
(2) J. Barr, R. J. Gillespie, R. Kapoor, and K. C. Malhotra, *Can. J. Chem.*, **46**, 149 (1968).
(3) D. J. Prince, J. D. Corbett, and B. Garbisch, *Inorg. Chem.*, **9**, 2731 (1970).
(4) I. D. Brown, D. B. Crump, and R. J. Gillespie, *Inorg. Chem.*, **10**, 2319 (1971).
(5) R. K. McMullan, D. J. Prince, and J. D. Corbett, *Inorg. Chem.*, **10**, 1749 (1971).
(6) N. J. Bjerrum, *Inorg. Chem.*, **9**, 1965 (1970).
(7) S. Dobinski and J. Wesolowski, *Bull. Int. Acad. Pol. Sci. Lett., Cl. Sci. Math. Nat., Ser. A*, 446 (1936).
(8) C. R. Boston, *J. Chem. Eng. Data*, **11**, 262 (1966).
(9) J. H. Simons, *J. Am. Chem. Soc.*, **52**, 3488 (1930).
(10) O. Hönigschmid and H. Baudrexler, *Z. Anorg. Allg. Chem.*, **223**, 91 (1935).
(11) C. B. Shoemaker and S. C. Abrahams, *Acta Crystallogr.*, **18**, 296 (1965).
(12) N. Trémillon and G. Letisse, *J. Electroanal. Chem.*, **17**, 371 (1968).
(13) L. G. Boxall, H. L. Jones, and R. A. Osteryoung, *J. Electrochem. Soc.*, **120**, 223 (1973).
(14) H. A. Oye, E. Rytter, P. Klaeboe, and S. J. Cyvin, *Acta Chem. Scand.*, **25**, 559 (1971).
(15) G. M. Begun, C. R. Boston, G. Torsi, and G. Mamantov, *Inorg. Chem.*, **10**, 886 (1971).
(16) J. Brynestad and G. P. Smith, *J. Phys. Chem.*, **72**, 296 (1968).
(17) J. H. von Barner, N. J. Bjerrum, and K. Kiens, *Inorg. Chem.*, **13**, 1708 (1974).
(18) L. R. Lieto, Thesis, 1969; Report ORNL-TM-2714, Oak Ridge National Laboratory, Oak Ridge, Tenn., 1969.
(19) K. Conrow, G. D. Johnson, and R. E. Bowen, *J. Am. Chem. Soc.*, **86**, 1025 (1964).
(20) IBM Application Program, System 1360 Scientific Subroutine Package, Version III, SE 13.
(21) See for example O. L. Davies and P. L. Goldsmith, "Statistical Methods in Research and Production", Oliver and Boyd, Edinburgh, 1972, pp 75, 134.
(22) R. J. Gillespie and P. K. Ummat, *Inorg. Chem.*, **11**, 1674 (1972).
(23) R. J. Gillespie, J. Passmore, P. K. Ummat, and O. C. Vaidya, *Inorg. Chem.*, **10**, 1327 (1971).
(24) R. Fehrmann, N. J. Bjerrum, and H. Andreasen, to be submitted for publication.

Contribution from the Department of Chemistry,
Polytechnic Institute of New York, Brooklyn, New York 11201

Bis(dimethylamido)tin(II). Synthesis and Characterization[1]

PAUL FOLEY and MARTEL ZELDIN*

Received July 31, 1974 AIC405267

Bis(dimethylamido)tin(II) is prepared by amination of anhydrous $SnCl_2$ with $LiN(CH_3)_2$. The compound is a white crystalline solid which is a dimer in cyclohexane solution and a monomer in the vapor phase. The compound reacts with alcohols to give $Sn(OR)_2$, with *N*-methyldiethanolamine to give $\overleftarrow{Sn(OCH_2CH_2)_2N}CH_2$, and with pyridine to give $[(CH_3)_2N]_2Sn\cdot py$. Ir and mass spectra are reported. The oxidation state of the compound is confirmed by calomel precipitation and Mössbauer isomer shift. Variable-temperature ^1H NMR spectra indicate exchange of the dimethylamido groups between bridge and terminal positions of a dimer structure.

Introduction

Compared to the other main group 4 elements, the chemistry of tin(II) compounds has been a relatively neglected area of research. Preparative and analytical difficulties arising from the ease of oxidation of the element in its lower oxidation state has been cited as the principal cause of inactivity in this field.[2] Hence perusal of the literature reveals only few well-characterized covalent tin(II) compounds. Particularly elusive has been the tin(II)–nitrogen bond. This bond has been proposed for several compounds (viz., bis(methyl-*N*-phenylcarbamate)tin(II)[3] and 2,2'-biphenylenedicarbamatotin(II)[4]) in short communications without significant supporting data.

The present study describes the high-yield synthesis of bis(dimethylamido)tin(II) and the unequivocal identification and characterization of the Sn^{II}–N bond by chemical and spectroscopic properties.

Experimental Section

All operations were carried out either in a dry oxygen-free nitrogen